The role of the tumor suppressor Lkb1 in energy homeostatis

Mans, L.A.

Chapter 4

Metabolic adaptation revealed: a transcriptome comparison of *lkb1* and wt larvae during yolk depletion and prolonged fasting

Laurie A. Mans [1], Gaetano Gargiulo [2] and Anna-Pavlina G. Haramis [1]

1 Institute of Biology, Leiden University, Sylviusweg 72, 2333 BE, Leiden, The Netherlands
2 Molecular Oncology, Max-Delbrück-Center for Molecular Medicine (MDC), Robert-Rössle-Str. 10, 13092 Berlin, Germany

Manuscript submitted

Abstract

Metabolic adaptation is important for the survival of an organism during times of varying nutrient availability or after disruption of the maternal nutrient supply. During the development of zebrafish larvae, metabolic adaptation occurs during yolk depletion. We have previously shown that zebrafish larvae mutated in *lkb1* fail to adapt their metabolism shortly after yolk depletion. To investigate the role of Lkb1 in the process of metabolic adaptation, we compared the transcriptomes of wild-type and *lkb1* larvae, before and after yolk depletion, and during prolonged fasting. We show that the expression profile of *lkb1* larvae after yolk depletion overlaps with that of wild-type larvae during prolonged fasting, thereby confirming a premature starvation state of *lkb1* larvae. Furthermore, we find that *lkb1* larvae show upregulation of *lepb, il6* and *il1b*, genes associated with cachexia pathophysiology. Finally, we find a gene set whose expression appears to be regulated directly by Lkb1 and independent of the presence of yolk, including unexpectedly, deregulation of the expression of several β- and γ-crystallin genes.

Introduction

Metabolism is a dynamic process that, amongst other factors, is regulated by nutrient availability. The ability to adapt to changing nutrient availability is crucial for an organism's survival. The molecular mechanisms associated with metabolic adaptation are intensively studied, but nonetheless only partly understood. Besides adaptation of an organism during times of (prolonged) fasting, a major point of metabolic adaptation occurs during birth, when maternal nutrient supply is depleted or interrupted. The metabolism of the neonate needs to adapt to this interruption and to the (composition of) external feeding. This metabolic adaptation was shown to be accompanied by induction of autophagy and gluconeogenesis (Girard, 1986). Disruption of these processes results in death of neonates shortly after birth (Kuma et al., 2004; She et al., 2000).

The zebrafish is a valuable model to study metabolism and metabolic adaptation. Many metabolic pathways are conserved between zebrafish and humans (Schlegel and Gut, 2015a). The externally fertilized embryos are supplied with nutrients from the yolk, which becomes depleted between 5 and 7 days post fertilization (dpf), after which, larvae start external feeding]. During yolk depletion, zebrafish larvae undergo metabolic adaptation, which is accompanied by activation of autophagy and of gluconeogenesis (Gut et al., 2013; Mans et al., 2017).

A critical regulator of metabolic adaptation is the serine-threonine kinase LKB1/STK11. LKB1 orchestrates many cellular processes, such as metabolism, cell growth and cell polarity, via the phosphorylation of downstream proteins such as AMPK and 12 other AMPK-related kinases (Shackelford and Shaw, 2009). Our group has previously shown that Lkb1 is crucial for the metabolic adaption during yolk depletion of zebrafish larvae, since *lkb1* larvae die shortly after yolk-depletion, whereas wild-type larvae can survive over a week longer. 7 dpf old *lkb1* larvae are characterized by low ATP levels, premature glycogen depletion, lipid accumulation in the liver (van der Velden et al., 2011), the lack of starvation-induced autophagy (Mans et al., 2017), and the premature upregulation of gluconeogenesis- and metabolic stress-related genes (unpublished data, Mans et al, 2018).

In this chapter, we characterize transcriptomic programs that are affected by depletion of Lkb1. We describe the gene expression profiles of wt larvae at 5, 7, before and after yolk depletion respectively, and 11 dpf, during prolonged fasting. These expression profiles were compared to those of *lkb1* larvae at 5 and 7 dpf, which is the maximum age at which all *lkb1* larvae are alive. Since we have previously shown that *lkb1* larvae are in a premature starvation state at 7 dpf, we compared the datasets of 7 dpf *lkb1* to 7 dpf wt to find genes that were differentially expressed.

To distinguish between genes whose expression is affected by prolonged fasting from those which are regulated directly by Lkb1, we compared the differentially expressed genes at 7 dpf (wt 7 dpf vs *lkb1* 7 dpf) to the dataset of differentially expressed genes during prolonged fasting (wt 7 dpf vs wt 11 dpf). Genes that are dysregulated in both datasets point to an indirect result of loss of Lkb1, whereas genes that are specifically dysregulated in *lkb1* larvae may be directly regulated by Lkb1. These Lkb1-associated genes could shed some light on the underlying mechanism of how Lkb1-deficiency leads to the inability to adapt metabolism upon metabolic challenge.

Results

Pre-data analysis reveals mature datasets that cluster by developmental time-point or genotype

To address the differences in gene expression profiles between *lkb1* larvae at 5 and 7 dpf, and wt larvae at 5,7 and 11 dpf, we performed mRNA sequencing on samples extracted from trunks only.

After sequencing, but before further data analysis, a quality control (QC) was performed to check the quality of all datasets (Figure 1A). The QC revealed that our datasets had minimal to no contamination with DNA, ribosomal RNA and mitochondrial DNA, and the vast majority of the reads were localized in exons. Therefore, we concluded that the libraries were clean, mature, antisense libraries that were suitable for further analysis.

To visualize how the datasets relate to each other we created a data cluster tree (Figure 1B). We found that in wt samples, the grouping factor is developmental time point; e.g. samples at 5 dpf group together, as do other time points. Interestingly, the first branch separates most *lkb1* samples from all wt samples, suggesting that in these *lkb1* samples genotype is a stronger grouping factor than developmental time point; *Lkb1* samples at 5 dpf group together with *lkb1* samples at 7 dpf rather than with wt samples at 5 dpf. There are, however, a few *lkb1* samples that cluster by developmental time-point rather than genotype.

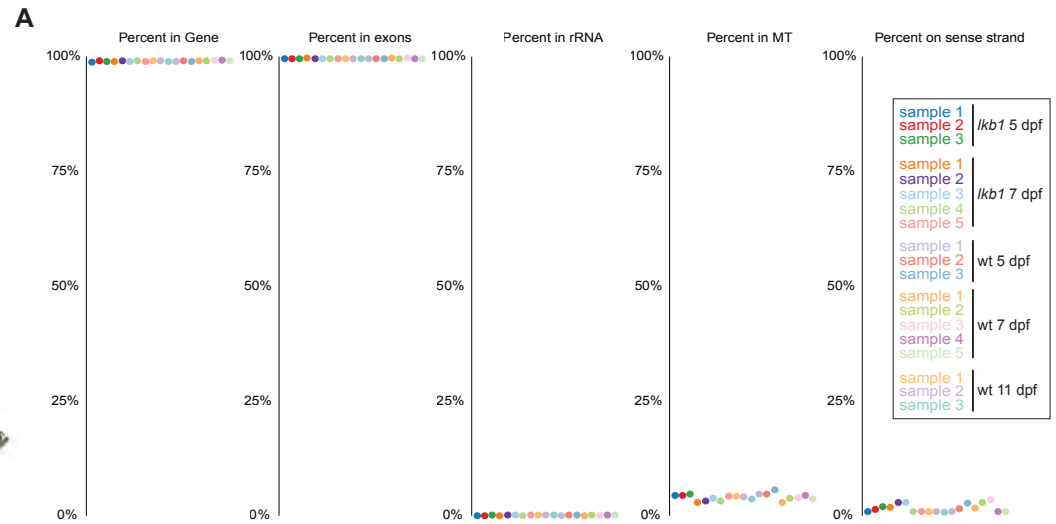

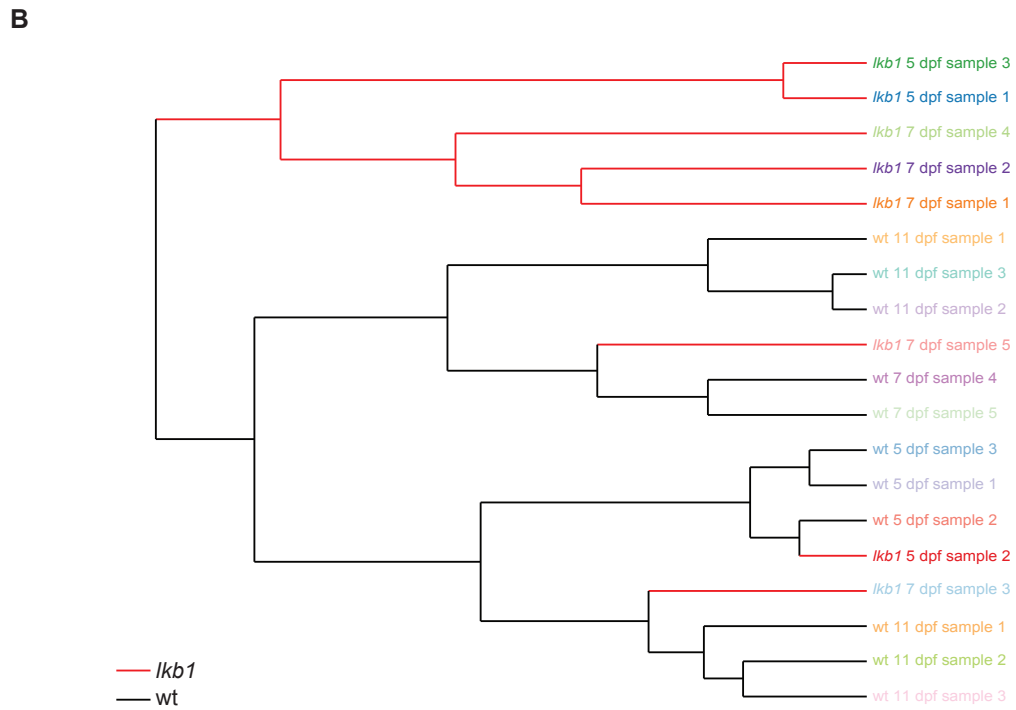

Figure 1. Quality control and cluster analysis. (A) Quality control of all samples. Most reads align to genes (percent in gene) and exons (percent in exon), which shows that all samples had little genomic DNA contamination and mature transcripts. The possible contamination of ribosomal RNA (rRNA) or mitochondrial (MT)RNA is shown as the percentage of rRNA and MT RNA. In all samples, both rRNA and MT RNA percentages were very low. Percent on sense strand depicts the direction of strand synthesis; in this case all reads are located on the antisense strand. Quality control of all samples was performed by SeqMonk. **(B)** Data cluster tree analysis. Wt samples group by developmental time-point. Most *lkb1* samples group separately from wt samples, revealing that genotype is a stronger grouping factor that developmental time-point. Samples were compared in SeqMonk, using a matrix calculated by Pearson correlation.

Differential gene expression analysis: Combining DESeq2, EdgeR and intensity difference filter

After the datasets were tested for quality, we compared differential gene expression between experimental groups. Depending on the research question, different pairwise comparisons can be chosen. For instance, to address the gene expression program that is associated with the feeding-fasting transition, wt samples of 5, 7 and 11 dpf can be compared. To investigate the gene expression program underlying the premature starvation state of *lkb1* larvae at 7 dpf, we compared the 7 dpf wt to 7 dpf *lkb1* using DESeq2 and EdgeR. As can be seen in Figure 2, using either DESeq2 (Figure 2A) or EdgeR (Figure 2B) gives different results. We chose to continue the analysis with genes whose expression levels were determined to be significant in both statistical tests. Furthermore, genes that are expressed at low levels might influence the differential expression analysis. For this reason, we used an additional analysis, the Intensity difference filter (Figure 2C). This filter corrects for number of reads, thereby giving more power to genes that are robustly expressed in both datasets, compared to genes that are very highly expressed in only one of the datasets. Combining the results of all three filters, resulted in a list of 114 genes out of a total of 26060 genes (Figure 2D). To validate the expression data, we performed qPCR on a subset of genes (Figure 2E).

Functional categorisation of differentially expressed genes reveals metabolism, eye development and immune system as most prevalent gene ontology groups.

We further categorized the list of differentially expressed genes by grouping them according to gene ontology. Strikingly, the most upregulated genes belong to the group of eye development (Figure 3A). Other highly represented groups are metabolism (Figure 3B), immunity (Figure 3C), and gene regulation and other cellular processes (Figure 3D). Apart from grouping by gene function, these figures also depict the expression levels of all tested groups, which provides the opportunity to assess how the expression of each gene changes during the period of metabolic adaptation and prolonged fasting.

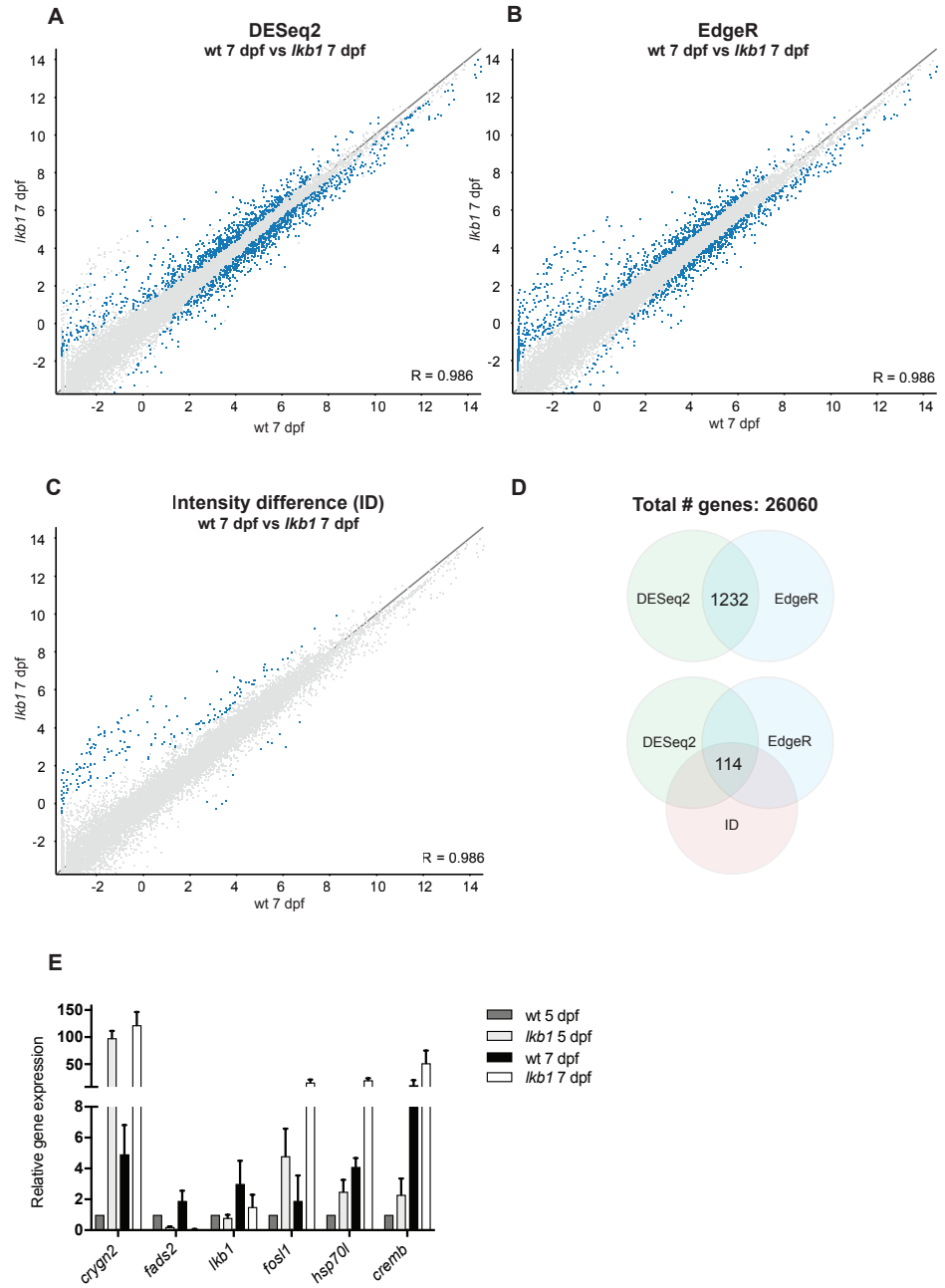

Figure 2. Differential gene expression between wt and *lkb1* larvae at 7 dpf. Differential gene expression analysis of total RNA isolated from trunks wt and *lkb1* larvae 7 dpf. 3 pipelines were used: **(A)** DESeq2, **(B)** EdgeR and **(C)** Intensity difference filter. Genes found differentially expressed in all pipelines **(D)**, were used for further analysis. FDR <0.05, P-value <0.05 and log2fold-change >1 were considered significant. **(E)** qPCR validation of *crygn2*, *fads2*, *lkb1*, *fosl1*, *hsp70l* and *cremb* in total RNA extracted from wt and *lkb1* trunks at 5 and 7 dpf. All genes match the expression pattern found in the RNAseq analysis. Data represent the means, relative to wt 5 dpf, ± standard errors of the means (SEM) and are pooled from three independent experiments.

A. Eye-related

name	wt 7 vs lkb1 7 (FC log2rpm)	wild-type 5 dpf	wild-type 7 dpf	wild-type 11 dpf	*lkb1* 5 dpf	*lkb1* 7 dpf	Description
crybb1l2	5,51	-1,68	-0,60	0,48	5,09	4,91	*crystallin, beta B1, like 2*
crygn2	5,49	-2,70	-1,17	-0,62	4,12	4,33	*crystallin, gamma N2*
cryba1l1	5,08	-1,43	-0,49	0,36	4,77	4,59	*crystallin, beta A1, like 1*
pdcb	4,99	-4,28	-3,79	-2,33	2,33	1,21	*phosducin b*
prph2a	4,96	-3,95	-3,64	-1,66	2,27	1,32	*peripherin 2a*
cryba1l2	4,65	-2,60	-3,29	-2,67	1,37	1,36	*crystallin, beta A1, like 2*
opn1sw2	3,98	-2,07	-1,57	-2,34	4,46	2,41	*opsin 1 (cone pigments), short-wave-sensitive 2*
gnat2	3,95	-0,87	-1,52	-1,22	5,01	2,43	*guanine nucleotide binding protein, alpha transducing activity,2*
sagb	3,94	1,51	-3,79	-3,94	3,10	0,16	*S-antigen; retina and pineal gland (arrestin) b*

B. Metabolism-related

name	wt 7 vs lkb1 7 (FC log2rpm)	wild-type 5 dpf	wild-type 7 dpf	wild-type 11 dpf	*lkb1* 5 dpf	*lkb1* 7 dpf	Description
lepb	4,82	-4,38	-4,16	-4,66	-3,40	0,65	*leptin b*
cyp46a	4,51	-3,04	-3,62	-4,08	0,74	0,90	*cytochrome p450, family 46, subfamily A, polypeptide 1*
pth1a	4,48	-3,95	-2,99	0,25	-2,39	1,49	*parathyroid hormone 1a*
lctla	3,95	-2,57	-3,16	-2,31	0,65	0,80	*lactase-like a*
scd	3,45	-0,30	-0,38	2,72	-0,73	3,07	*stearoyl-coa desaturase (delta-9-desaturase)*
camkk1	3,36	-2,43	-1,63	-1,28	0,55	1,73	*calcium/calmodulin-dependent protein kinase kinase 1, alpha*
pomca	3,29	-2,26	-2,49	1,07	0,53	0,80	*proopiomelanocortin a*
cart3	3,28	-0,93	-0,40	-0,75	-0,15	2,88	*cart3*
odc1	2,34	5,14	4,26	4,97	4,89	6,60	*ornithine decarboxylase 1*
cyp46a1	2,31	3,49	0,25	0,89	3,84	2,55	*cytochrome p450, family 46, subfamily A, polypeptide 1*
me1	2,21	4,08	1,57	0,75	4,37	3,78	*malic enzyme 1*, NADP(+)-dependent, cytosolic
tdh2	2,19	0,88	1,48	2,49	2,83	3,67	*l-threonine dehydrogenase 2*
igfbp1a	1,99	6,11	7,39	8,94	7,40	9,37	*insulin-like growth factor binding protein 1a*
gpx1b	1,81	4,92	5,90	5,97	6,43	7,71	*glutathione peroxidase 1b*
pfkfb3	1,19	4,70	4,85	4,56	5,33	6,04	*6-phosphofructo-2-kinase/fructose-2,6-biphosphatase3*
elovl2	-1,81	5,14	4,12	4,15	4,25	2,31	*elongation of very long chain fatty acids-like 2*
fads2	-2,74	5,03	5,18	5,02	3,28	2,44	*fatty acid desaturase 2*
apoa4	-3,06	3,50	2,48	1,58	2,45	-0,58	*apolipoprotein a-IV*

Figure 3. Transcriptome analysis reveals starvation-related and Lkb1-regulated expression patterns. Transcriptome analysis of total RNA isolated from trunks wt and *lkb1* larvae at 5, 7 dpf and wt at 11 dpf. **(A)** Heatmap of genes associated with eye function and development. **(B)** Heatmap of genes associated with metabolic processes. (next page) **(C)** Heatmap of regulatory genes associated with various cellular processes. **(D)** Heatmap of genes associated with other cellular processes. Data represents fold change of log2rpm.

C. Immunity

name	wt 7 vs lkb1 7 (FC log2rpm)	wild-type 5 dpf	wild-type 7 dpf	wild-type 11 dpf	*lkb1* 5 dpf	*lkb1* 7 dpf	Description
calca	1,66	2,70	2,81	3,28	3,71	4,48	*calcitonin/calcitonin-related polypeptide, alpha*
plac8.2	4,53	-3,04	0,06	4,24	-1,00	4,58	*placenta-specific 8, tandem duplicate 2*
ponzr4	2,59	0,14	0,42	1,09	2,89	3,01	*plac8 onzin related protein 4*
ponzr3	2,24	2,01	1,87	2,73	4,02	4,11	*plac8 onzin related protein 3*
gtpbp1	2,19	4,66	4,26	5,72	4,82	6,46	*gtp binding protein 1*
il11a	4,20	-2,93	-3,70	-1,83	-2,77	0,49	*interleukin 11a*
hbz	4,18	-0,91	-1,14	-2,02	2,23	3,04	*hemoglobin zeta*
il1b	2,83	-1,01	0,28	0,33	-0,34	3,11	*interleukin 1, beta*
c7 (2 of 2)	2,58	2,34	3,29	5,33	3,36	5,88	*complement component 7*
isg15	2,48	-1,79	-0,67	2,56	-1,38	1,81	*isg15 ubiquitin-like modifier*
junbb	2,46	3,85	4,31	5,69	4,89	6,77	*jun b proto-oncogene b*
itln3	2,41	2,53	0,76	3,62	3,68	3,17	*intelectin 3*
junba	2,13	2,66	3,84	4,41	3,94	5,96	*jun b proto-oncogene a*
bcl6ab	2,01	2,28	1,68	2,88	3,28	3,70	*b-cell cll/lymphoma 6a, genome duplicate b*
crp	1,99	5,32	1,66	-0,02	5,81	3,65	*c-reactive protein, pentraxin-related*
mpx	1,98	4,00	3,76	5,44	4,11	5,74	*myeloid-specific peroxidase*
btg2	1,96	4,84	5,45	6,04	6,29	7,41	*B-cell translocation gene 2*
il6st	1,22	3,08	2,41	3,75	3,51	3,63	*interleukin 6 signal transducer*
cd74a	-1,99	0,92	2,92	2,41	0,54	0,93	*cd74 molecule, major histocompatibility complex*
hpx	-3,04	4,22	2,22	-1,08	3,21	-0,82	*hemopexin*

D. Other cellular processes

name	wt 7 vs lkb1 7 (FC log2rpm)	wild-type 5 dpf	wild-type 7 dpf	wild-type 11 dpf	*lkb1* 5 dpf	*lkb1* 7 dpf	Description
spsb2	5,22	-3,70	-3,19	-0,88	-1,12	2,03	*spla/ryanodine receptor domain and socs box containing 2*
foxg1b	4,60	-1,96	-1,87	0,62	2,14	2,73	*forkhead box g1b*
ankrd1b	4,44	0,85	-0,71	-1,78	1,52	3,74	*ankyrin repeat domain 1b*
faim2	4,30	-3,42	-4,13	-3,22	-0,29	0,17	*fas apoptotic inhibitory molecule 2*
capn3a	4,10	-1,40	-1,79	-2,50	3,52	2,30	*calpain 3a, (p94)*
mcm5	3,85	-1,43	-1,66	-0,09	-0,83	2,20	*mcm5 minichromosome maintenance deficient 5 (S. cerevisiae)*
fosl1a	3,67	0,15	0,19	2,70	1,32	3,86	*fos-like antigen 1a*
hsp70l	3,49	0,35	0,55	2,38	1,09	4,04	*heat shock cognate 70-kd protein, like*
ndrg1b	3,46	-0,35	-0,03	0,44	1,67	3,43	*n-myc downstream regulated gene 1b*
gc3	3,26	-3,04	-2,21	0,42	1,41	1,05	*guanylyl cyclase 3*
crem (2 of 2)	3,07	-0,76	-0,56	0,86	1,06	2,51	*camp responsive element modulator*
hspb9	2,72	2,90	3,25	4,38	3,78	5,96	*heat shock protein, alpha-crystallin-related, 9*
plek2	2,51	1,21	0,43	0,22	1,93	2,94	*pleckstrin 2*
dpagt1	2,50	3,52	2,79	4,96	3,61	5,29	*upd-n-acetylglucosamine, glcnAc-1-p transferase*
cabz01040055	2,10	4,16	3,13	3,97	3,32	5,23	*three-finger protein 5*
smad6a	2,06	3,85	3,27	3,32	5,51	5,33	*smad family member 6a*
snx10a	2,05	2,33	1,08	0,95	2,43	3,13	*sorting nexin 10a*
atf3	2,03	3,29	3,88	5,22	3,63	5,91	*activating transcription factor 3*
crem (1 of 2)	1,97	4,87	5,06	6,29	6,24	7,03	*camp responsive element modulator*
oaz2b	1,92	2,08	2,38	3,30	3,34	4,30	*ornithine decarboxylase antizyme 2b*
fos	1,90	3,66	4,59	5,24	5,72	6,49	*v-fos fbj murine osteosarcoma viral oncogene homolog*
npas4a	1,87	2,50	3,86	5,41	4,68	5,74	*neuronal pas domain protein 4a*
slc26a3	1,80	6,30	5,26	5,46	7,37	7,07	*solute carrier family 26 (anion exchanger), member 3*
dusp5	1,80	1,60	1,92	2,51	2,94	3,72	*dual specificity phosphatase 5*
csrnp1a	1,80	2,84	2,94	4,21	3,70	4,74	*cysteine-serine-rich nuclear protein 1a*
rhbdd1	1,76	1,45	2,12	3,14	1,67	3,88	*rhomboid domain containing 1*
ier2	1,72	1,63	2,27	2,66	2,76	3,99	*immediate early response 2*
cep55l	1,68	3,60	2,68	3,88	5,38	4,35	*centrosomal protein 55 like*
dnajb9b	1,67	2,89	2,49	3,68	2,57	4,16	*dnaj (hsp40) homolog, subfamily B, member 9b*
slc16a9a	1,65	4,15	4,87	4,99	5,00	6,52	*solute carrier family 16 (monocarbox. acid transporters)*, 9a
tmem41ab	1,61	3,49	2,62	1,98	4,00	4,23	*transmembrane protein 41ab*
syt13	1,59	2,82	2,64	3,26	4,19	4,23	*synaptotagmin XIII*

Metabolic deregulation and cachexia-associated expression profile in *lkb1* larvae

The list of metabolism-related genes provides insight into the metabolic status of *lkb1* larvae through time, and likely distinguishes genes that are deregulated as a result of the premature starvation, from Lkb1-regulated genes. As expected, we found genes with a similar expression profile in 7dpf *lkb1* and 11 dpf wt samples, confirming the premature starvation state of *lkb1* larvae (Figure 3). Interestingly, there are also genes, whose expression is changed only in 7dpf *lkb1* samples, implying that they regulated by Lkb1 under metabolic stress.

The most highly upregulated gene in the group of metabolism-related genes is *leptin b* (*lepb*), which encodes for leptin, a peripheral hormone that regulates the control of feeding, glucose metabolism and energy expenditure (Figure 3B). Leptin b is the true ortholog of mammalian Leptin (Michel et al., 2016). Leptin was identified in mammalian adipocytes (Halaas et al., 1995) and is well characterized in mice and humans. Its expression rises after feeding, resulting in the inhibition of food intake via its anorexigenic properties. There are some differences in leptin physiology among vertebrates. For instance, in zebrafish, as in other fish species, leptin is mainly produced in the liver, and plays a role in the regulation of pancreatic β-cell mass and glucose homeostasis but not in adipostasis or feeding behavior (Michel et al., 2016). The expression of leptin in response to feeding or fasting, however, has not been investigated in zebrafish. *Lepb* is highly overexpressed in *lkb1* larvae compared to wts at all time-points examined. High leptin expression in a "starved" state is intriguing, as in mammals leptin levels decrease during fasting (Ahima et al., 1996) and indeed, *lepb* was not upregulated in starved wt larvae at 11 dpf.

Interestingly, genes implicated in *lepb* signalling were also differentially expressed in *lkb1* larvae. Leptin binding to the Leptin receptor (LR) in the hypothalamus leads to suppression of food intake through inhibition of neuropeptide Y (NYP) neurons and stimulation of proopiomelanocortin (POMC) and cocaine- and amphetamine-regulated transcript (CART) neurons (Ahima and Hileman, 2000; Elias et al., 1998; Volkoff, 2016). We found both *pomca* and *cart3* upregulated in 7 dpf *lkb1* compared to 7 dpf wt larvae (Figure 3B). While the increase of *pomca* and *cart3* has been previously described in starved wt zebrafish (Akash et al., 2014; Shanshan et al., 2016), we found only *pomca* upregulated in wt larvae at 11 dpf.

A (pathological) setting where leptin is overexpressed and the organism is under severe metabolic stress is in wasting syndrome, or cachexia (Engineer and Garcia, 2012). Cachexia is characterized by general weight-loss, severe muscle mass loss, and systemic inflammation. Cachexia is associated with an increase in mRNA levels of *Leptin, UCP2, IL-1β* and *IL-6* in various tissues such as muscle, heart and liver (Argiles et al., 2013; Sanchis et al., 1998). We measured the mRNA levels of *leptin* and the cachexia-associated genes in *lkb1* and wt larvae at 7 dpf, and the expression of all these markers was highly upregulated in *lkb1* larvae with *lepb* being over 30x times overexpressed (Figure 4). These results indicate that *lkb1* larvae exhibit a pathophysiology that resembles that of cachexia.

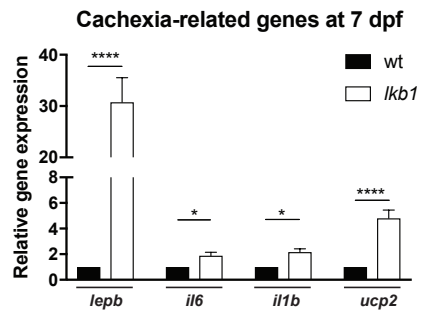

Figure 4. Cachexia-related genes are overexpressed in *lkb1* larvae. Gene expression analysis of *lepb*, il-6 and *il1β* in total RNA extracted from wt and *lkb1* trunks at 7 dpf. All genes were significantly upregulated in *lkb1* samples compared to wt. *Lepb* expression is dramatically upregulated (30x) in *lkb1* samples compared to wt. Data represent the means, ± standard errors of the means (SEM) and were obtained from samples of three independent experiments. Each sample contained 10 pooled larvae from a single-paired mating. * P-value <0.02, **** P-value <0.005; two-tailed student's t-test.

Expression of *β- and γ-crystallins* is dramatically upregulated in *lkb1* larvae

Amongst the eye development-related genes we found the expression of several crystallin genes to be upregulated (Figure 3A). Interestingly, although crystallins are typically lens proteins, expression of crystallins has been shown outside the lens, in tissues such as heart, kidney, liver, skeletal muscle, and lung (Dubin et al., 1989; Lee et al., 2005; Srinivasan et al., 1992). Interestingly, many crystallin protein families show structural similarities to small heat-shock proteins, detoxifying enzymes and metabolic enzymes, such as lactate dehydrogenase and a-enolase (Andley, 2008). For instance, intensive research on α-crystallins has revealed that they function as molecular chaperones, and exhibit pro-apoptotic and enzymatic properties in other tissues than the lens (reviewed in (Andley, 2008)). These alternative functions and locations led to the proposition that crystallins might have originated via gene-recruitment or co-option (Kim and Wistow, 1993; True and Carroll, 2002). In zebrafish, 3 α-, 13 β- and 37 γ-crystallins have been identified (Greiling et al., 2009) and extensive literature has established the zebrafish as a valuable model to study crystallins in various biological contexts (Archer et al., 2012; Mishra et al., 2018; Parolini et al., 2018; Pinto et al., 2016).

We found that β- and γ-crystallins, namely, *crybb1l2* (crystallin β B1, like 2), *crygn2* (crystallin γ N2) and *cryba1l1* and *cryba1l2* (crystallin β A1, like 1 and 2) were differentially expressed (Figure 3A). Although much research has been done on α-crystallins, less is known about the β- and γ-crystallins. Interestingly, these genes are highly expressed in *lkb1* trunks at both 5 and 7 dpf, implying that their expression is not associated with yolk depletion. For most eye development genes, we observed a slight increase in expression upon yolk depletion, and during prolonged fasting in wild-type samples (*crybb1l2, crygn2, cryba1l1, pdcb, prph2a*), but not as high as in *lkb1* samples (Figure 3A).

Subset of Lkb1-regulated genes are deregulated prior to yolk-depletion

We next aimed to identify genes whose expression is directly regulated by Lkb1, independently of yolk depletion. We performed correlation clustering to select differentially expressed genes in *lkb1* larvae compared to wt larvae, at both 5 and 7 dpf. We found both up- and downregulated genes (Figure 5A, B), but the upregulated genes showed a much higher level of differential expression. For a more detailed view of the expression of these *lkb1*-specific genes in the different samples, we drew a graph in which gene expression changes can be followed in all the samples (Figure 5C). Interestingly, this graph reveals that some *lkb1* samples are not following the "expression profile" of other *lkb1* samples, but rather that of wt samples. Nonetheless, all the genes from this list are only highly overexpressed in *lkb1* samples and not in wt samples at any time-point. Therefore, we can still assume that these genes are upregulated as a direct result of the loss of Lkb1.

This list includes several of the previously mentioned β- and γ-crystallins. This confirms that crystallins, together with the other genes from this list, are indeed deregulated independently of yolk depletion and only in *lkb1* larvae. The cause of this deregulation could be explained by direct regulation by Lkb1, or indirectly by a different Lkb1-regulated pathway. Either way, the deregulation of these genes provides insight into the effect of whole-body Lkb1 depletion and new possible pathways via which Lkb1 regulates essential biological processes such as metabolism.

A

			wild-type			*lkb1*		
name	wt 5 vs *lkb1* 5 (FC log2rpm)	wt 7 vs *lkb1* 7 (FC log2rpm)	5 dpf	7 dpf	11 dpf	5 dpf	7 dpf	Description
crygn2	6,82	5,49	-2,70	-1,17	-0,62	4,12	4,33	*crystallin, gamma n2*
crybb1l2	6,77	5,51	-1,68	-0,60	0,48	5,09	4,91	*crystallin, beta b1, like 2*
pdcb	6,61	4,99	-4,28	-3,79	-2,33	2,33	1,21	*phosducin b*
opn1sw2	6,52	3,98	-2,07	-1,57	-2,34	4,46	2,41	*opsin 1, short-wave-sensitive 2*
prph2a	6,22	4,96	-3,95	-3,64	-1,66	2,27	1,32	*peripherin 2a*
cryba1l1	6,21	5,08	-1,43	-0,49	0,36	4,77	4,59	*crystallin, beta A1, like 1*
gnat2	5,89	3,95	-0,87	-1,52	-1,22	5,01	2,43	*guanine nucleotide binding protein*
capn3a	4,92	4,10	-1,40	-1,79	-2,50	3,52	2,30	*calpain 3a, (p94)*
cryba1l2	3,96	4,65	-2,60	-3,29	-2,67	1,37	1,36	*crystallin, beta A1, like 2*
cyp46a1	3,77	4,51	-3,04	-3,62	-4,08	0,74	0,90	*cytochrome P450, family 46, subfamily A, 1*
lctla	3,22	3,95	-2,57	-3,16	-2,31	0,65	0,80	*lactase-like a*
hbz	3,13	4,18	-0,91	-1,14	-2,02	2,23	3,04	*hemoglobin zeta*
faim2	3,13	4,30	-3,42	-4,13	-3,22	-0,29	0,17	*fas apoptotic inhibitory molecule 2*
camkk1	2,99	3,36	-2,43	-1,63	-1,28	0,55	1,73	*calc/calmodulin-dependent protein kinase 1, alpha*
ponzr4	2,76	2,59	0,14	0,42	1,09	2,89	3,01	*plac8 onzin related protein 4*

B

cr925813.2	-1,78	-2,27	1,27	1,82	2,07	-0,51	-0,46	*Uncharacterized*
fads2	-1,76	-2,74	5,03	5,18	5,02	3,28	2,44	*fatty acid desaturase 2*
zgc:112146	-1,23	-1,86	5,56	4,94	3,37	4,33	3,09	*zgc:112146*
apoa4	-1,04	-3,06	3,50	2,48	1,58	2,45	-0,58	*apolipoprotein a-IV*

Figure 5. Cluster analysis pinpoint *Lkb1*-regulated expression profiles. Cluster analysis of total RNA isolated from trunks wt and *lkb1* larvae at 5, 7 dpf and wt at 11 dpf.
Heatmap of genes upregulated in *lkb1* samples at 5 and 7 dpf. **(B)** Heatmap of genes downregulated in *lkb1* samples at 5 and 7 dpf. Data represent fold change of log2rpm. (Next page) **(C)** Expression profiles of Lkb1-regulated genes per sample.

C

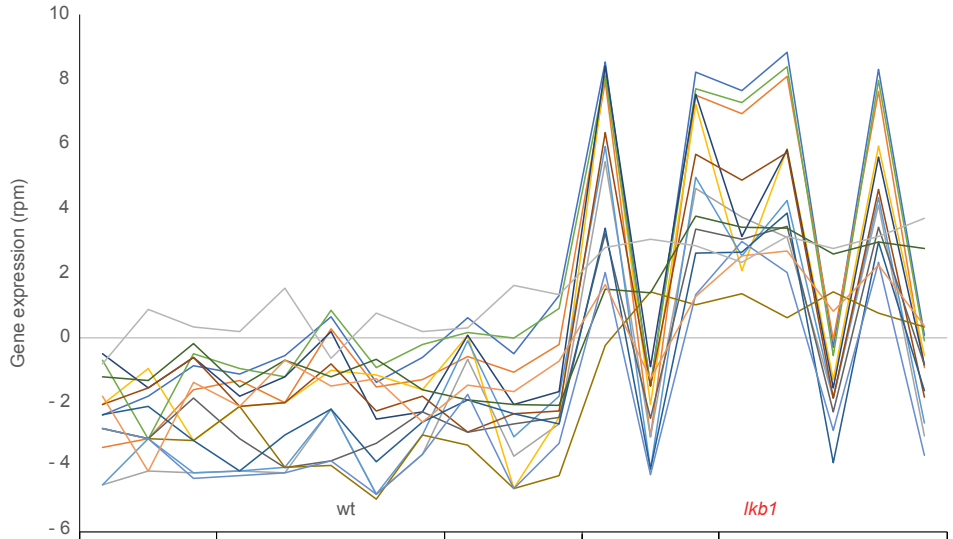

	5 dpf			7 dpf			11 dpf			5 dpf			7 dpf				
crybb1l2	-2.39	-1.81	-0.86	-1.11	-0.55	0.66	-1.38	-0.60	0.61	-0.48	1.30	8.53	-1.48	8.22	7.66	8.83	-0.28	8.30	0.07
crygn2	-3.39	-3.13	-1.59	-1.31	-2.01	0.29	-1.51	-1.28	-0.59	-1.07	-0.21	7.92	-3.07	7.50	6.93	8.09	-0.06	7.61	-0.93
pdcb	-4.54	-4.13	-4.18	-4.11	-4.17	-2.21	-4.83	-3.60	-0.66	-3.65	-2.67	5.45	-3.07	4.62	3.72	3.11	-1.87	4.12	-3.04
opn1sw2	-2.07	-0.96	-3.18	-2.11	-2.01	-0.99	-1.13	-1.60	0.09	-4.65	-2.45	8.23	-2.07	7.21	2.08	5.86	-1.28	5.94	-0.54
prph2a	-4.54	-3.13	-4.18	-4.11	-4.01	-2.21	-4.83	-3.02	-0.10	-3.07	-1.80	5.92	-4.07	4.97	2.54	4.26	-1.87	4.32	-2.63
cryba1l1	-0.69	-3.13	-0.48	-0.95	-1.21	0.84	-0.93	-0.21	0.18	-0.01	0.91	8.11	-1.48	7.70	7.27	8.38	-0.55	7.97	-0.10
gnat2	-0.48	-1.54	-0.59	-1.79	-1.21	0.20	-2.51	-2.28	0.09	-2.07	-1.67	8.41	-0.90	7.53	3.13	5.81	-1.55	5.59	-0.82
capn3a	-2.07	-1.54	-0.59	-2.11	-2.01	-0.80	-2.25	-1.79	-2.91	-2.33	-2.26	6.35	-1.48	5.69	4.87	5.74	-1.87	4.59	-1.82
cryba1l2	-2.80	-3.13	-1.86	-3.11	-4.01	-3.80	-3.25	-2.28	-2.91	-2.65	-2.45	3.22	-2.48	3.36	3.05	3.45	-2.28	3.42	-0.82
cyp46a1	-2.80	-3.13	-3.18	-2.11	-4.01	-3.95	-4.99	-3.02	-3.33	-4.65	-4.26	-0.24	1.42	1.02	1.36	0.63	1.42	0.75	0.33
lctla	-2.39	-2.13	-3.18	-4.11	-3.01	-2.21	-3.83	-2.60	-1.91	-2.33	-2.67	3.40	-4.07	2.62	2.66	3.86	-3.87	2.98	-1.63
hbz	-1.22	-1.32	-0.18	-1.53	-0.69	-1.21	-0.66	-1.60	-1.91	-2.07	-2.09	1.52	1.39	3.77	3.43	3.39	2.61	2.98	2.77
faim2	-2.80	-3.13	-4.33	-4.27	-4.17	-3.80	-4.83	-3.60	-1.74	-4.65	-3.26	2.01	-4.22	1.33	2.98	2.03	-2.87	2.34	-3.63
camkk1	-1.80	-4.13	-1.37	-2.11	-0.69	-1.48	-1.25	-2.60	-1.45	-1.65	-0.73	1.65	-1.26	1.27	2.52	2.69	0.83	2.26	0.37
ponzr4	-0.80	0.87	0.34	0.21	1.54	-0.63	0.78	0.21	0.30	1.63	1.34	2.79	3.04	2.86	2.33	3.12	2.77	3.13	3.70

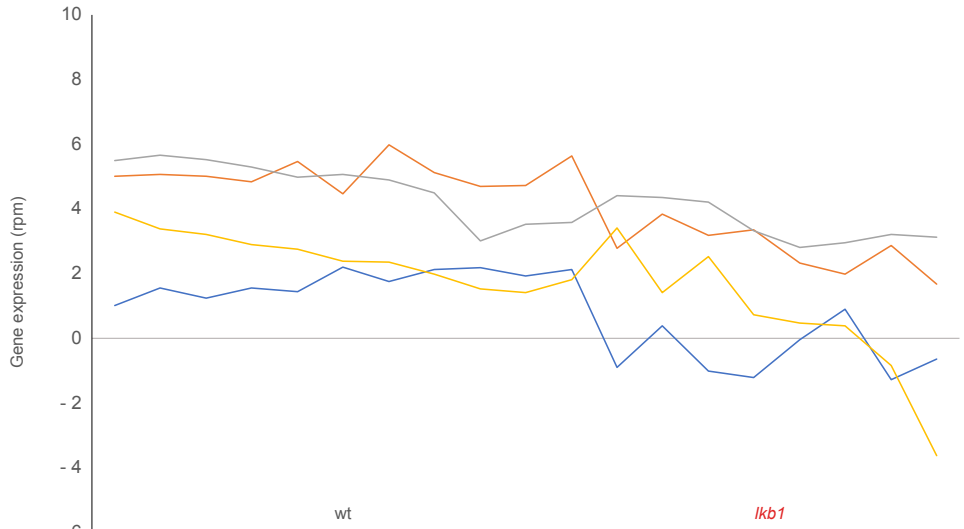

	5 dpf			7 dpf			11 dpf			5 dpf			7 dpf				
cr925813	1.00	1.54	1.25	1.56	1.45	2.20	1.75	2.13	2.18	1.92	2.13	-0.91	0.39	-1.02	-1.22	-0.03	0.89	-1.28	-0.63
fads2	5.00	5.08	5.02	4.84	5.46	4.48	5.98	5.14	4.68	4.73	5.65	2.79	3.85	3.19	3.34	2.34	1.99	2.86	1.68
zgc:112146	5.50	5.66	5.52	5.30	4.97	5.06	4.89	4.49	3.00	3.53	3.57	4.41	4.36	4.22	3.34	2.81	2.95	3.21	3.13
apoa4	3.90	3.37	3.22	2.91	2.77	2.39	2.35	1.98	1.53	1.41	1.80	3.42	1.42	2.53	0.72	0.47	0.38	-0.83	-3.63

Discussion

The tumor suppressor LKB1 is a key regulator of metabolism. To further unravel the role of Lkb1 in metabolic adaptation we used an *lkb1* zebrafish model. *Lkb1* zebrafish larvae present with premature starvation at around 6 days post fertilization (dpf), soon after yolk depletion, and die between 7 and 8 dpf, whereas non-fed wt larvae can survive over a week after yolk depletion, and exhibit characteristics of starvation at around 11 dpf. To investigate the effect of Lkb1 depletion on whole-body energy homeostasis we compared the transcriptomes of wt and *lkb1* larvae at 5 and 7 days post fertilization, and prolonged fasted wt larvae at 11 dpf. We focussed on genes that were differentially expressed between *lkb1* and wt larvae at 7 dpf, to gain insight into the role of Lkb1 in metabolic adaptation. Furthermore, these data gave us the opportunity to distinguish differentially expressed genes that are similarly expressed in wt during prolonged fasting, from genes that are specifically deregulated in *lkb1* larvae.

We compared the genes that were differentially expressed between *lkb1* and wt larvae at 7 dpf, and grouped them according to biological function. The most prevalent gene ontology groups were metabolism, eye function and development, immunity, and gene regulation along with other cellular processes. We demonstrate that *lkb1* larvae exhibit significant upregulation of *leptin* expression. The zebrafish Leptin b is a true ortholog of mammalian Leptin (Michel et al., 2016). Leptin was identified in mammalian adipocytes (Halaas et al., 1995) and is well characterized in mice and humans. Its expression rises after feeding, resulting in the inhibition of food intake via its anorexigenic properties. There are some differences in leptin physiology among vertebrates. For instance, in zebrafish, as in other fish species, leptin is mainly produced in the liver, and plays a role in the regulation of pancreatic β-cell mass and glucose homeostasis but not in adipostasis or feeding behaviour (Michel et al., 2016). The expression of leptin in response to feeding or fasting, however, has not been investigated in zebrafish. *Lepb* is highly overexpressed in *lkb1* larvae compared to wt at all time-points examined. High leptin expression in a “starved” state is intriguing, as in mammals leptin levels decrease during fasting (Ahima et al., 1996) and indeed, *lepb* was not upregulated in starved wt larvae at 11 dpf. Furthermore, we demonstrate that *lkb1* larvae exhibit significant upregulation of pro-inflammatory cytokines *il-1b* and *il-6*, which are associated with cachexia. Deregulation of systemic metabolism and increased inflammation are molecular characteristics associated with wasting syndrome/cachexia. Thus, the zebrafish *lkb1* model may be useful to study molecular interplay of systemic metabolism and inflammation that are deregulated in cachexia.

Since we isolated RNA from trunks, it was unexpected to find genes that are associated with eye function and development being highly upregulated in these tissues. However, a more comprehensive search of the crystallin family revealed various locations of expression and alternative functions. For instance, it was shown that exposure of zebrafish to cocaine or its metabolites resulted in upregulation of 3 β and 3 γ-crystallins (Parolini et al., 2018). They proposed that this could be an organismal response to the stress due to the cocaine exposure. Other studies found that expression of γ-crystallins decreased upon activation of the Liver X receptor (LXR) by antagonists (Archer et al., 2012; Pinto et al., 2016). These studies highlight the possible functions of crystallins outside the lens and eye tissue, and implicate putative functions of crystallins in the response to stress. An upregulation of crystallins in *lkb1* larvae as a response to stress is plausible, since we have shown that they exhibit an exacerbated fasting response and up-regulation of markers associated with metabolic stress such as *fgf21, ucp2 and lpin1* (Mans et al., submitted). However, the upregulation of these stress-markers and the premature starvation of *lkb1* larvae manifest only after yolk depletion, whereas the overexpression of crystallins is already observed at 5 dpf. To expand the analysis into the function of crystallins, and other genes that are regulated by *lkb1*; it would be interesting to assess their expression levels through time to evaluate when deregulation occurs, and to pinpoint their role in the *lkb1* metabolic phenotype in zebrafish larvae, and possibly in other Lkb1-deficient models. Another notable gene in the list of upregulated genes in *lkb1* larvae only, is *calpain 3 (capn3)* (Figure 5). Calpain 3 is characterized as a skeletal muscle-specific cysteine protease (Sorimachi et al., 1989)1989, but is also expressed in lens and retina tissue (Greiling et al., 2009; Herasse et al., 1999). It belongs to the calpain family, which are calcium-dependent intracellular proteases, also referred to as modulator proteases (Ono et al., 2016) since they modify their substrates rather than degrade them. In humans, overexpression of calpains results in various pathologies such as neurodegenerative and cardiovascular disorders, ischaemia, cancers and cataracts (Ono et al., 2016). Interestingly, calpains inhibit autophagy (Williams et al., 2008), and *lkb1* larvae lack starvation-induced autophagy as a means to restore energy homeostasis upon yolk depletion. Indeed, treatment with calpeptin (a calpains' inhibitor and autophagy-inducing compound) restored autophagy in *lkb1* larvae and prolonged their lifespan (Mans et al., 2017).

Overall, this study provides a detailed analysis of the effects of whole-body Lkb1 depletion on the regulation of various transcriptional programs. We confirm the previously described premature starvation state by identifying transcriptional profiles in *lkb1* larvae that resemble profiles of prolonged fasted wild-type larvae.

Finally, we also identified genes that are specifically dysregulated in *lkb1* larvae, providing new insights in the transcriptional programs that are (directly) regulated by Lkb1.

Material and methods

Zebrafish strains and Screening Methods

Zebrafish were handled in compliance with the local animal welfare regulations and were maintained according to standard protocols (zfin.org). Their culture was approved by the local animal welfare committee (DEC) of the University of Leiden and all protocols adhered to the international guidelines specified by the EU Animal Protection Directive 2010/63/EU. Genotype analysis for *lkb1*-mutant embryos was performed with SNP-specific PCR analysis.

RNA extraction for transcriptome analysis

Trunks of embryos from single-paired matings were individually stored in RNAlater (Invitrogen, AM7021) until genotyped. Total RNA was isolated from 10 trunks of either *lkb1* or wt trunks, with the RNaqueous micro Total RNA isolation kit (Thermo Fisher Scientific, AM-1931) following manual. Briefly, 10 trunks were lysed in 200 ul Lysis solution, supplemented with 100 ul 100% EtOH and applied to the column. Total mRNA was eluted in 2x10 ul Elution solution concentrations were measured using the Nanodrop (ND-1000).

Transcriptome analysis

Total RNA isolated from trunks of 5, 7 dpf wt and *lkb1* larvae, and 11 dpf wt larvae were analysed in triplo using an Illumina sequencing pipeline. The 51-bp single-end reads were mapped to the Danio rerio genome (Zv9) using TopHat (2.0.12) (Trapnell et al., 2009). Statistical analysis was performed using the online platform SeqMonk (Babraham Bioinformatics). The differential expression of genes was determined using the build-in scripts for DESeq2 (Love et al., 2014) and EdgeR (Robinson et al., 2010). A False Discovery Rate (FDR) for differential expression lower than 0.05, P-values lower than 0.05 and a log2 fold-change more than 1 were considered significant.

Gene expression analysis

To validate the sequencing results, qPCR was performed for *lkb1* (Liver kinase b 1, ENSDARG00000046074, fw- acagcatcccggaggagt, rev-caggatcatattccagcattcc),

crygn2 (crystalline gamma N2, ENSDARG00000030411, fw-tggtagctgggtggcttatg, rev- cagtgtaagcaggaaccacg), cremb (cAMP responsive element modulator b, ENSDARG00000102899, fw-ccgactgatgaagaacaggac, rev-cgtctctaaacccagcacatagt), *fads2* (fatty acid desaturase 2, ENSDARG00000019532, fw-gtgcctgctgagacgtgata, rev-cacccactggctgacgttat), *fosl1* (FOS-like antigen 1, ENSDARG00000015355, fw-gcacaacccaacaacaacag, rev-ctggtttgacgttatggcatt), *hsp70l* (heatshock protein 70, like, ENSDARG00000055723, fw-ccgacgaggtgtttattcg, rev-acacccccacacaggagtag).

To examine expression of cachexia-associated genes the following primers were used. *il1b* (interleukin 1 beta, ENSDARG00000098700, fw-gaacagaatgaagcacatcaaacc, rev-acggcactgaatccaccac), *il6* (interleukin 6, ENSDARG00000102318, fw-tcaacttctccagcgtgatg, rev-tctttccctcttttcctcctg), *lepb* (Leptin b, ENSDARG00000045548, fw-attgctcgaaccaccatcag, rev-gatgtcagggccaaatcaa), *ucp2* (uncoupling protein 2, ENSDARG00000043154, fw-ctgatgactgatgatcttccct, rev-tgacgaacataaccacattcc), as housekeeping gene we used primers against *ppiaa* (ENSDARG00000009212, fw- acactgaaacacggaggcaaag, rev-catccacaaccttcccgaacac).

For qPCR analysis 500-1000 ng of total RNA was reverse transcribed using iScript cDNA synthesis kit (BioRad, 1708890). 1:10 Diluted cDNA was analysed with real-time quantitative RT-PCR performed in a Bio-Rad CFX96 system. Primer sequences for other reactions are shown in Supp. Table 2. Data analysis of qPCR results represents data from three independent experiments. Error bars represent the means ± standard errors of the means (SEM). Statistical significance was calculated using 2way ANOVA using a Tukey's multiple comparisons test.

References

Ahima, R.S., and Hileman, S.M. (2000). Postnatal regulation of hypothalamic neuropeptide expression by leptin: implications for energy balance and body weight regulation. Regul Pept *92*, 1-7.

Ahima, R.S., Prabakaran, D., Mantzoros, C., Qu, D., Lowell, B., Maratos-Flier, E., and Flier, J.S. (1996). Role of leptin in the neuroendocrine response to fasting. Nature *382*, 250-252.

Akash, G., Kaniganti, T., Tiwari, N.K., Subhedar, N.K., and Ghose, A. (2014). Differential distribution and energy status-dependent regulation of the four CART neuropeptide genes in the zebrafish brain. J Comp Neurol *522*, 2266-2285.

Andley, U.P. (2008). The lens epithelium: focus on the expression and function of the alpha-crystallin chaperones. Int J Biochem Cell Biol *40*, 317-323.

Archer, A., Venteclef, N., Mode, A., Pedrelli, M., Gabbi, C., Clement, K., Parini, P., Gustafsson, J.A., and Korach-Andre, M. (2012). Fasting-induced FGF21 is repressed by LXR activation via recruitment of an HDAC3 corepressor complex in mice. Mol Endocrinol *26*, 1980-1990.

Argiles, J.M., Lopez-Soriano, F.J., and Busquets, S. (2013). Mechanisms and treatment of cancer cachexia. Nutr Metab Cardiovasc Dis *23 Suppl 1*, S19-24.

Dubin, R.A., Wawrousek, E.F., and Piatigorsky, J. (1989). Expression of the murine alpha B-crystallin gene is not restricted to the lens. Mol Cell Biol *9*, 1083-1091.

Elias, C.F., Lee, C., Kelly, J., Aschkenasi, C., Ahima, R.S., Couceyro, P.R., Kuhar, M.J., Saper, C.B., and Elmquist, J.K. (1998). Leptin activates hypothalamic CART neurons projecting to the spinal cord. Neuron *21*, 1375-1385.

Engineer, D.R., and Garcia, J.M. (2012). Leptin in anorexia and cachexia syndrome. Int J Pept *2012*, 287457.

Girard, J. (1986). Gluconeogenesis in late fetal and early neonatal life. Biol Neonate *50*, 237-258.
Greiling, T.M., Houck, S.A., and Clark, J.I. (2009). The zebrafish lens proteome during development and aging. Mol Vis *15*, 2313-2325.

Gut, P., Baeza-Raja, B., Andersson, O., Hasenkamp, L., Hsiao, J., Hesselson, D., Akassoglou, K., Verdin, E., Hirschey, M.D., and Stainier, D.Y. (2013). Whole-organism screening for gluconeogenesis identifies activators of fasting metabolism. Nat Chem Biol *9*, 97-104.

Halaas, J.L., Gajiwala, K.S., Maffei, M., Cohen, S.L., Chait, B.T., Rabinowitz, D., Lallone, R.L., Burley, S.K., and Friedman, J.M. (1995). Weight-reducing effects of the plasma protein encoded by the obese gene. Science *269*, 543-546.

Herasse, M., Ono, Y., Fougerousse, F., Kimura, E., Stockholm, D., Beley, C., Montarras, D., Pinset, C., Sorimachi, H., Suzuki, K., et al. (1999). Expression and functional characteristics of calpain 3 isoforms generated through tissue-specific transcriptional and posttranscriptional events. Mol Cell Biol *19*, 4047-4055.

Kim, R.Y., and Wistow, G.J. (1993). Expression of the duck alpha-enolase/tau-crystallin gene in transgenic mice. FASEB J *7*, 464-469.

Kuma, A., Hatano, M., Matsui, M., Yamamoto, A., Nakaya, H., Yoshimori, T., Ohsumi, Y., Tokuhisa, T., and Mizushima, N. (2004). The role of autophagy during the early neonatal starvation period. Nature *432*, 1032-1036.

Lee, F.Y., Kast-Woelbern, H.R., Chang, J., Luo, G., Jones, S.A., Fishbein, M.C., and Edwards, P.A. (2005). Alpha-crystallin is a target gene of the farnesoid X-activated receptor in human livers. J Biol Chem *280*, 31792-31800.

Love, M.I., Huber, W., and Anders, S. (2014). Moderated estimation of fold change and dispersion for RNA-seq data with DESeq2. Genome biology *15*, 550.

Mans, L.A., Querol Cano, L., van Pelt, J., Giardoglou, P., Keune, W.J., and Haramis, A.G. (2017). The tumor suppressor LKB1 regulates starvation-induced autophagy under systemic metabolic stress. Sci Rep *7*, 7327.

Michel, M., Page-McCaw, P.S., Chen, W., and Cone, R.D. (2016). Leptin signalling regulates glucose homeostasis, but not adipostasis, in the zebrafish. Proceedings of the National Academy of Sciences of the United States of America *113*, 3084-3089.

Mishra, S., Wu, S.Y., Fuller, A.W., Wang, Z., Rose, K.L., Schey, K.L., and McHaourab, H.S. (2018). Loss of alphaB-crystallin function in zebrafish reveals critical roles in the development of the lens and stress resistance of the heart. J Biol Chem *293*, 740-753.

Ono, Y., Saido, T.C., and Sorimachi, H. (2016). Calpain research for drug discovery: challenges and potential. Nat Rev Drug Discov *15*, 854-876.

Parolini, M., Bini, L., Magni, S., Rizzo, A., Ghilardi, A., Landi, C., Armini, A., Del Giacco, L., and Binelli, A. (2018). Exposure to cocaine and its main metabolites altered the protein profile of zebrafish embryos. Environ Pollut *232*, 603-614.

Pinto, C.L., Kalasekar, S.M., McCollum, C.W., Riu, A., Jonsson, P., Lopez, J., Swindell, E.C., Bouhlatouf, A., Balaguer, P., Bondesson, M., et al. (2016). Lxr regulates lipid metabolic and visual perception pathways during zebrafish development. Mol Cell Endocrinol *419*, 29-43.

Robinson, M.D., McCarthy, D.J., and Smyth, G.K. (2010). edgeR: a Bioconductor package for differential expression analysis of digital gene expression data. Bioinformatics *26*, 139-140.

Sanchis, D., Busquets, S., Alvarez, B., Ricquier, D., Lopez-Soriano, F.J., and Argiles, J.M. (1998). Skeletal muscle UCP2 and UCP3 gene expression in a rat cancer cachexia model. FEBS Lett *436*, 415-418.

Schlegel, A., and Gut, P. (2015). Metabolic insights from zebrafish genetics, physiology, and chemical biology. Cell Mol Life Sci *72*, 2249-2260.

Shackelford, D.B., and Shaw, R.J. (2009). The LKB1-AMPK pathway: metabolism and growth control in tumour suppression. Nat Rev Cancer *9*, 563-575.

Shanshan, L., Cuizhen, Z., and Gang, P. (2016). Effects of starvation on the expression of feeding related neuropeptides in the larval zebrafish hypothalamus. Yi chuan = Hereditas *38*, 821-830.

She, P., Shiota, M., Shelton, K.D., Chalkley, R., Postic, C., and Magnuson, M.A. (2000). Phosphoenolpyruvate carboxykinase is necessary for the integration of hepatic energy metabolism. Mol Cell Biol *20*, 6508-6517.

Sorimachi, H., Imajoh-Ohmi, S., Emori, Y., Kawasaki, H., Ohno, S., Minami, Y., and Suzuki, K. (1989). Molecular cloning of a novel mammalian calcium-dependent protease distinct from both m- and mutypes. Specific expression of the mRNA in skeletal muscle. J Biol Chem *264*, 20106-20111.

Srinivasan, A.N., Nagineni, C.N., and Bhat, S.P. (1992). alpha A-crystallin is expressed in non-ocular tissues. J Biol Chem *267*, 23337-23341.

Trapnell, C., Pachter, L., and Salzberg, S.L. (2009). TopHat: discovering splice junctions with RNA-Seq. Bioinformatics *25*, 1105-1111.

True, J.R., and Carroll, S.B. (2002). Gene co-option in physiological and morphological evolution. Annu Rev Cell Dev Biol *18*, 53-80.

van der Velden, Y.U., Wang, L., Zevenhoven, J., van Rooijen, E., van Lohuizen, M., Giles, R.H., Clevers, H., and Haramis, A.P. (2011). The serine-threonine kinase LKB1 is essential for survival under energetic stress in zebrafish. Proc Natl Acad Sci U S A *108*, 4358-4363.

Volkoff, H. (2016). The Neuroendocrine Regulation of Food Intake in Fish: A Review of Current Knowledge. Front Neurosci *10*, 540.

Williams, A., Sarkar, S., Cuddon, P., Ttofi, E.K., Saiki, S., Siddiqi, F.H., Jahreiss, L., Fleming, A., Pask, D., Goldsmith, P., et al. (2008). Novel targets for Huntington's disease in an mTOR-independent autophagy pathway. Nat Chem Biol *4*, 295-305.